Membrane lipid patterns typify distinct anaerobic methanotrophic consortia

Martin Blumenberg*, Richard Seifert*†, Joachim Reitner‡, Thomas Pape*, and Walter Michaelis*

*Institute of Biogeochemistry and Marine Chemistry, University of Hamburg, Bundesstrasse 55, 20146 Hamburg, Germany; and ‡Geowissenschaftliches Zentrum, University of Göttingen, Goldschmidtstrasse 3, 37077 Göttingen, Germany

The anaerobic oxidation of methane (AOM) is one of the major sinks of this substantial greenhouse gas in marine environments. Recent investigations have shown that diverse communities of anaerobic archaea and sulfate-reducing bacteria are involved in AOM. Most of the relevant archaea are assigned to two distinct phylogenetic clusters, ANME-1 and ANME-2. A suite of specific ^{13}C-depleted lipids demonstrating the presence of consortia mediating AOM in fossil and recent environments has been established. Here we report on substantial differences in the lipid composition of microbial consortia sampled from distinct compartments of AOM-driven carbonate reefs growing in the northwestern Black Sea. Communities in which the dominant archaea are from the ANME-1 cluster yield internally cyclized tetraether lipids typical of thermophiles. Those in which ANME-2 archaea are dominant yield sn-2-hydroxyarchaeol accompanied by crocetane and crocetenes. The bacterial lipids from these communities are also distinct even though the sulfate-reducing bacteria all belong to the *Desulfosarcina*/*Desulfococcus* group. Nonisoprenoidal glycerol diethers are predominantly associated with ANME-1-dominated communities. Communities with ANME-2 yield mainly conventional, ester-linked diglycerides. ANME-1 archaea and associated sulfate-reducing bacteria seem to be enabled to use low concentrations of methane and to grow within a broad range of temperatures. Our results offer a tool for the study of recent and especially of fossil methane environments.

U p to 90% of the methane produced in anoxic marine sediments and waters is oxidized anaerobically (1–3). Several studies (e.g., ref. 4) have shown that the process involves both anaerobic archaea and sulfate-reducing bacteria (SRB), with electrons being transferred from methane to sulfate. Two phylogenetically distinct groups of archaea, termed ANME-1 and ANME-2, are involved (5). Organisms from both archaeal groups can assimilate methane. *In vitro*, consortia based on ANME-2 oxidize methane at higher specific rates than those based on ANME-1 (6–8). Microscopy shows that ANME-2 archaea are closely associated with SRB partners (9), whereas ANME-1 cells often occur as monospecific aggregates (5, 8). To date, factors favoring one of these consortia over the other are not understood. Accordingly, tools that can reveal distributions of these consortia in recent and fossil environments are important to studies of microbial ecology and biogeochemical mechanisms.

The Black Sea is the world's largest reservoir of dissolved methane, with concentrations as high as ≈15 μmol/liter (10). Anaerobic oxidation of methane (AOM) is important both in sediments and in the water column (11, 12). Bioherms up to 4 m high and with diameters of 50 cm are found on the seafloor (8). The archaea in consortia from the massive inner parts of these structures are from the ANME-1 group (8, 13). However, despite the quantitative predominance of ANME-1 cells in a previously described mat (8), ongoing microbial and biomarker investigations have shown that the sample used for biomarker analyses includes minor amounts of ANME-2 archaea (sample C; see Table 1). All portions of these structures yield microbial lipids that are strongly depleted in ^{13}C (δ^{13}C $<$ $-70‰$) and thus reflect utilization of methane as carbon source, but lipid com-

positions and microbial populations are apparently covariant. We show here that specific lipids associated with ANME-1-dependent or ANME-2-dependent consortia can be recognized.

Materials and Methods

Sample Collection. Samples were collected during summer 2001 in the northwestern Black Sea (44°46.5′N, 31°59.6′E, GHOSTDABS field) at a water depth of 230 m by using the manned submersible Jago off board the research vessel Professor Logachev. Lipid biomarkers were analyzed from distinct mat types, and subsamples were used for molecular microbiological analyses. The samples for lipid investigations were kept at $-20°C$ until analyses. Local position and denotation of mat types are given in Fig. 1.

Analysis of Lipid Biomarkers. The wet mat samples (3–10 g wet weight) were saponified in 6% KOH in methanol (75°C, 3 h) and extracted with *n*-hexane to yield the neutral lipids. Carboxylic acid methyl esters were obtained by acidification of the residual phase to pH 1, extraction with CH_2Cl_2, and subsequent methylation using trimethylchlorosilane in methanol (1/8, vol/vol; 2 h at 70°C). Positions of double bonds within methyl esters of unsaturated fatty acids were determined by mass spectrometric analyses of dimethyldisulfide derivatives and coelution experiments with authentic standards. The neutral lipids were separated by thin-layer chromatography (silica gel 60, 0.25 mm, CH_2Cl_2) into (*i*) diols and polyols such as glycerol monoethers and cyclic tetraethers (R_f = 0–0.1); (*ii*) alcohols, including glycerol diethers (R_f = 0.1–0.35); and (*iii*) apolar compounds, including hydrocarbons (R_f = 0.35–1). An aliquot of the hydrocarbon fraction was hydrogenated at room temperature in a sealed vial by using Pd on charcoal as catalyst. The alcohols were silylated with N,O-bis(trimethylsilyl)trifluoroacetamide (BSTFA) for 1 h at 80°C before analysis. To analyze ether-containing lipids, aliquots of the fractions *i* and *ii* were combined and subjected to ether cleavage through HI treatment (2 h at 110°C) and reduction of the resulting iodides by using LiAlH$_4$ and LiAlD$_4$ in dry diethyl ether under an argon atmosphere (modified after ref. 14). Compounds were analyzed by combined gas chromatography/mass spectrometry (HP6890 gas chromatograph coupled to a Micromass Quattro II mass spectrometer) and identified by comparison of mass spectra and retention times with published data and/or reference compounds [in particular, crocetane synthetic standard (provided by S. Rowland, School of Earth, Ocean and Environmental Sciences, University of Plymouth, Plymouth, U.K.); crocetenes (15); saturated and unsaturated 2,6,10,15,19-pentamethylicosanes (16, 17); archaeol (2,3-di-*O*-phytanyl-*sn*-glycerol) (18); *sn*-2-hydroxyarchaeol (2-*O*-3-hydroxyphytanyl-3-*O*-phytanyl-*sn*-glycerol) (19);
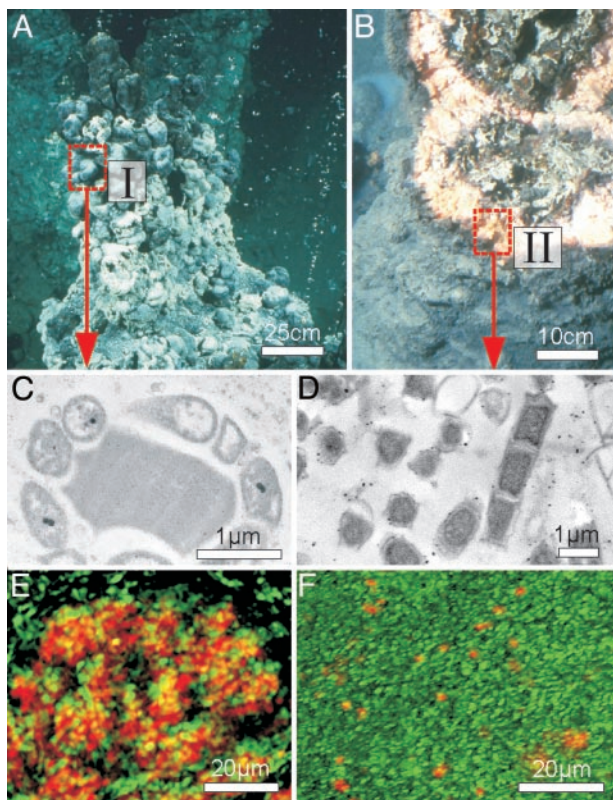
MICROBIOLOGY

Fig. 1. Images of a chimney-like structure combined with results of molecular microbiological investigations. (*A*) Chimney-like structure growing in the anoxic waters of the Black Sea (230 m water depth). Predominating black parts of the gas- and water-filled globules are at the top (mat type I). (*B*) Part of a broken microbial structure with the massive pink-orange predominating mat (mat type II). The interior of the bioherms consists of gray-greenish porous carbonate. (*C* and *D*) Images obtained by transmission electron microscopy (TEM) from mat type I and mat type II, respectively. (*E*) Fluorescence *in situ* hybridization (FISH) of mat type I (probes: EelMS932 (ANME-2), fluorescence green; *Desulfosarcina/Desulfococcus* group DSS658cy3, fluorescence red). (*F*) FISH of mat type II (probes: ANME-1, fluorescence green; *Desulfosarcina/Desulfococcus* group DSS658cy3, fluorescence red). For technical details see *Materials and Methods*. Note the lesser abundance of SRB in the ANME-1 association compared with the ANME-2 association.

biphytane authentic standards obtained from *Sulfolobus solfataricus* (provided by G. Antranikian, Institute of Technical Microbiology, Technische Universität Hamburg-Harburg); and 1,2-di-*O*-12-methyltetradecyl-*sn*-glycerol (20)].

$\delta^{13}C$ values of lipids were measured (minimum of three replications) by using a ThermoFinnigan Trace GC (GC-C-IRMS) gas chromatograph coupled to a Finnigan MAT 252 isotope-ratio mass spectrometer. The combustion reactor contained CuO, Ni, and Pt and was operated at 940°C. The stable carbon isotope compositions are reported in the delta notation ($\delta^{13}C$) vs. the Vienna Pee Dee belemnite standard. Isotopic compositions of alcohols and fatty acids were corrected for addition of trimethylsilyl groups and the addition of the carbon atom during the preparation of methyl esters.

TEM and FISH. Samples for TEM were fixed with 4% buffered glutardialdehyde and postfixed with 2% OsO_4. Thin sections of microbial mats were cut by using a Leica hardpart Microtome. Image stacks with a *Z* spacing of 0.25 μm were obtained by using a piezomover (Physik Instrumente, Waldbronn, Germany) attached to a Plan-Apochromat ×63 objective (Zeiss; numerical aperture = 1.4) of a Zeiss Axioplan microscope. Image process-

ing was carried out by using the METAMORPH imaging software (Universal Imaging, West Chester, PA) and the EPRTM deconvolution software (Scanalytics, Billerica, MA) (21). Paraffin sections of decalcified samples were stained with various histochemicals, namely toluidine blue O, alcian blue, several oligonucleotide probes for FISH, and 4′,6-diamidino-2-phenylindole (DAPI) for DNA detection. 16S rRNA oligonucleotide probes were used with a stringency of 40–60%. Six sections of each mat type were analyzed. Oligonucleotides were purchased 5′-labeled with the indocarbocyanine dye Cy3 (CyDye; Amersham Pharmacia Biotech) and Oregon green (Molecular Probes) from Biometra (Göttingen, Germany) and Metabion (Ebersberg, Germany). All oligonucleotides were stored in TE buffer (10 nM Tris/1 mM EDTA, pH 7.5) at −20°C. Working solutions were adjusted to 50 ng of DNA per μl. Prewarmed hybridization solution [0.9 M NaCl/20 mM Tris·HCl, pH 7.2/0.01% SDS/35% (vol/vol) formamide] was mixed with fluorescently labeled oligonucleotide (1 ng per μl of hybridization solution). The following gene probes were used: DSS658 (22), ANME-1 (9), EelMS932 (ANME-2) (9), and Cren499 (23). Glutardialdehyde-fixed samples were dried with Peldri II (Pelco, Redding, CA) to avoid drying artifacts. TEM investigations were carried out with a Zeiss EM 10 instrument at 60–80 kV.

Results

Morphology of the Black Sea Structures. Fig. 1*A* illustrates the morphology of the microbial structures found. The chimney-like constructions are mainly composed of globules filled with gas and water at the top (black predominating part, mat type I) and a quantitatively prevailing massive pink-orange part (mat type II, up to 10 cm in diameter; Fig. 1*B*).

Lipid Differences of the Black Sea Mat Types. Biomarker compositions differed strongly between mat types I and II. Both contained ^{13}C-depleted saturated and unsaturated homologues of the irregular isoprenoid 2,6,10,15,19-pentamethylicosane (PMI) with up to five double bonds ($\delta^{13}C = -107.1$ to $-111.5‰$). Crocetane (2,6,11,15-tetramethylhexadecane; e.g., sample A $\delta^{13}C = -105‰$) and crocetenes (up to two double bonds; $\delta^{13}C = -108.6‰$; Fig. 2) were found only in mat type I. Type I mats also contained C_{20}-isoprenoidal glycerol diethers, with concentrations of *sn*-2-hydroxyarchaeol (2-*O*-3-hydroxyphytanyl-3-*O*-phytanyl-*sn*-glycerol; e.g., sample A $\delta^{13}C = -102.3‰$) exceeding those of archaeol (2,3-di-*O*-phytanyl-*sn*-glycerol, $\delta^{13}C = -98.7‰$) by a factor of 5 or more (Fig. 2*A*). In contrast, hydroxyarchaeols are almost absent from type II mats (Fig. 2*B*). Glycerol dialkyl glycerol tetraethers (GDGTs) constitute the majority of archaeal lipids in type II mats (Fig. 3*B*; e.g., sample F $\delta^{13}C = -91‰$) but are undetectable in type I mats (Fig. 3*A*). Biphytanes with three or more internal rings (cyclopentyl or cyclohexyl) are absent from both mat types. Inputs from pelagic *Crenarchaeota* (24) are, therefore, insignificant.

Profiles of bacterial lipids also differ markedly in type of glycerol linkage and composition (Fig. 4). Type I mats yield mainly ester-linked fatty acids with C16:1ω7 (e.g., sample A $\delta^{13}C = -83.3‰$), the uncommon C16:1ω5 ($\delta^{13}C = -84.5‰$), and cycC17:0ω5,6 ($\delta^{13}C = -85.1‰$) predominating [fatty acid:monoalkyl glycerol monoether:dialkyl glycerol diether (FA:MAGE:DAGE) ratio of the main aliphatic structure in sample A = 79:14:7]. Bacterial lipids from the type II mats are dominantly ether-linked, with mainly terminally branched 12-methyltetradecane structures (e.g., in sample F *ai*-C15:0 DAGE; $\delta^{13}C = -83.5‰$; *ai*-C15:0; $\delta^{13}C = -78.9‰$; FA:MAGE:DAGE ratio of the main aliphatic structure = 48:1:51).

Absolute concentrations of selected biomarkers subsequent to alkaline hydrolysis, showing that prokaryotic lipids are much more abundant in sample A than in sample F, are given in Table 1 and Fig. 4.
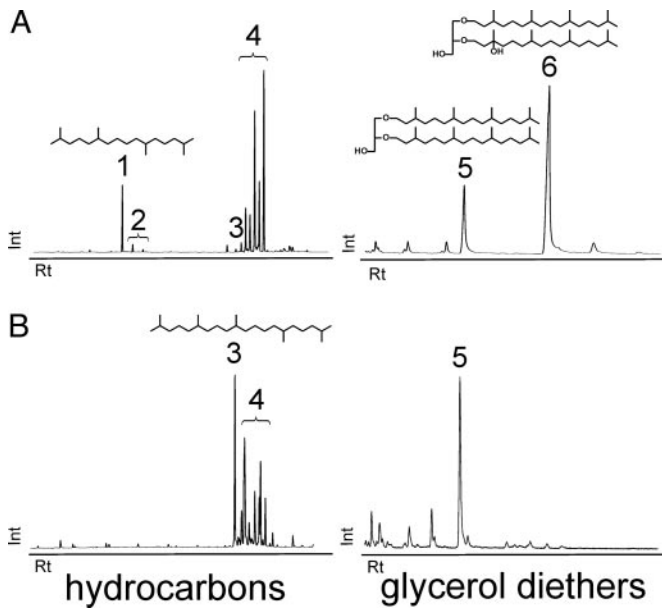
Blumenberg *et al.*

Fig. 2. Distributions of archaeal isoprenoidal hydrocarbons and glycerol diethers in compartments of the chimney-like structures (mat type I with ANME-2 as predominant methanotrophs and the ANME-1-dominated mat type II). Shown are reconstructed partial ion chromatograms of strongly ^{13}C-depleted lipids (δ^{13}C < −78‰). Int, intensity; Rt, retention time. (*A*) Isoprenoidal hydrocarbons and glycerol diethers obtained from mat type I. (*B*) Isoprenoidal hydrocarbons and glycerol diethers of the mat type II. Alcohols from alkaline hydrolysis [measured as *N,O*-bis(trimethylsilyl)trifluoro-acetamide (BSTFA) derivatives]. Peaks: 1, crocetane (2,6,11,15-tetramethyl-hexadecane); 2, unsaturated crocetanes with up to two double bonds; 3, PMI (2,6,10,15,19-pentamethylicosane); 4, unsaturated PMIs with up to five double bonds; 5, archaeol (2,3-di-*O*-phytanyl-*sn*-glycerol); and 6, *sn*-2-hydroxyarchaeol (2-*O*-3-hydroxyphytanyl-3-*O*-phytanyl-*sn*-glycerol).

TEM and FISH. Samples of both mat types were examined by using TEM and FISH. Close associations of two cell types were observed within the type I mat (Fig. 1*C*), where microorganisms of spherical shape (1–2 μm) are closely surrounded by smaller cells (0.5 μm). FISH data revealed that this association consists of ANME-2 methanotrophs (Fig. 1*E*; fluorescence green) and SRB belonging to the *Desulfosarcina/Desulfococcus* group (Fig. 1*E*; red fluorescence). These consortia form aggregates of variable size. Archaea of the ANME-1 group are almost absent. In contrast, filamentous, cylindrical cells (up to 10 μm in length; Fig. 1*D*) are dominant in the massive pink-orange mat (type II). Applications of gene probes identified these cells as archaea of the ANME-1 cluster (Fig. 1*F*; green fluorescence) also accompanied by SRB of the *Desulfosarcina/Desulfococcus*-group but in lesser abundance compared to mat type I (Fig. 1F; red fluorescence). Application of a specific probe provided no evidence of a significant contribution of members of the *Crenarchaeota* to the microbial population of either mat type.

Discussion

Distinction Between ANME-1 and ANME-2 by Biomarkers. The strikingly distinct lipid profiles observed in this work offer a means for rapidly surveying populations of methane-consuming microorganisms. The ANME-1 and -2 groups of archaea are distinguished by the abundance ratios of *sn*-2-hydroxyarchaeol to archaeol and of total biphytanes to phytane (after cleavage of ether bonds). The presence of crocetane and crocetenes is also diagnostic for ANME-2 archaea. Examples of data are shown in Table 1. Samples A and F (Figs. 2 and 3) represent end members. Samples B–E represent cases in which, although one type of consortium is dominant, both types are present. High relative
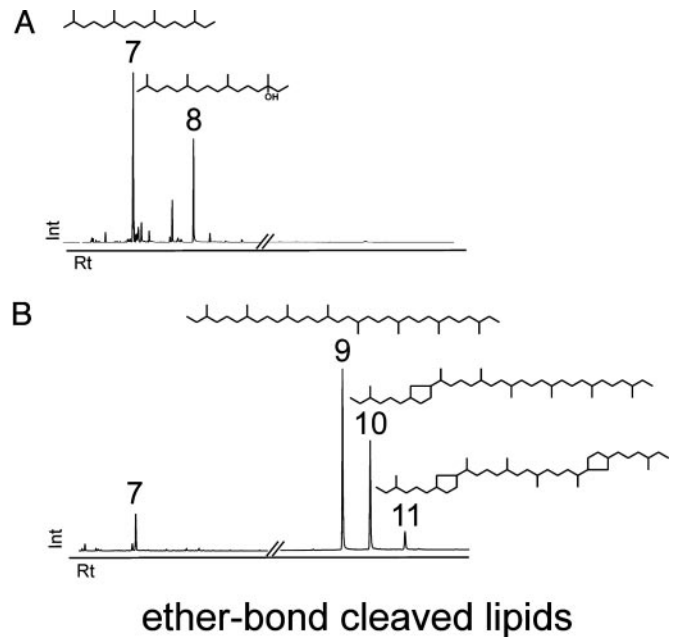
Fig. 3. Biomarker distributions of mat type I (ANME-2-dominated) and mat type II (ANME-1-dominated) obtained from the cleavage of ether bonds. (*A*) Lipids of the black parts of the gas-filled globules from the top of the structures (mat type I). (*B*) Products of ether bond cleavage from the massive pink-orange mat (mat type II). Peaks: 7, phytane (3,7,11,15-tetramethylhexadecane); 8, hydroxyphytane (3-hydroxy-3,7,11,15-tetramethylhexadecane); 9, C40:0 (3,7,11,15,18,22,26,30-octamethyldotriacontane); 10, C40:1 [1-(1,5,8,12,16,20-hexamethyldocosyl)-3-(4-methylhexyl)-cyclopentane]; 11, C40:2 {1,1′-(1,5,8,12-tetramethyl-1,12-dodecandiyl)-bis[3-(4-methylhexyl)]-cyclopentane}.

amounts of *sn*-2-hydroxyarchaeol and the lack or very low abundance of tetraether lipids in the more exposed mat type I indicate that ANME-2 are the predominating methanotrophic archaea in compartments with comparatively high methane partial pressure and free gas venting off the sediment. In contrast, mats with lipid compositions similar to those of sample F (mat type II, with ANME-1 as the most abundant archaea) are dominant in the massive, inner, more secluded parts.
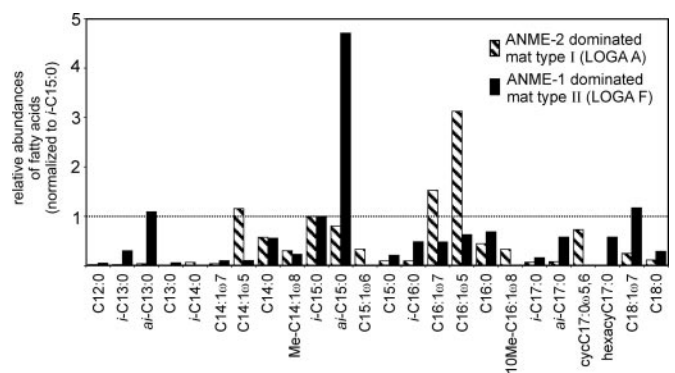
Fig. 4. Fatty acid patterns of bacteria (mainly SRB of the *Desulfosarcina/Desulfococcus* cluster) of mat types dominated by ANME-1 and ANME-2. The occurrences are normalized to the 13-methyltetradecanoic acid (*i*-C15:0). The ANME-1-dominated sample (mat type II) shows high concentrations of terminally branched bacterial fatty acids with the *ai*-C15:0 predominating. The SRB associated with the ANME-2 (mat type I) are mainly composed of hexadecenoic acids with C16:1ω5 as the major component. The relatively high abundance of cycC17:0ω5,6 in ANME-2-associated bacteria is lacking in microorganisms thriving in the ANME-1-ruled mat. The concentrations of *i*-C15:0 are 891 μg per g of dry mat in sample A and 39 μg per g of dry mat in sample F.

Table 1. Ratios of selected lipid components of different samples corresponding to two mat types and absolute and relative amounts of archaeal isoprenoids

Sample	Type	Major groups of archaea and SRB identified*	(arch + OH-arch)/arch − 1	(phy + Σbiph)/phy − 1	Conc., μg per g dry weight (δ^{13}C in ‰ vs. VPDB)						
					arch	OH-arch	Σbiph	croc	crocΔ	PMI	PMIΔ
A	I	ANME-2/DSS	5.5	0.0	821 (−99)	4517 (−102)	ND (NA)	98 (−105)	+	9 (−98)	+++
B	I	ANME-2 (ANME-1)/DSS	1.4	0.5	222 (−101)	311 (−103)	262 (NA)	62 (−108)	+	13 (−105)	+++
C	II	ANME-1 (ANME-2)/DSS†	0.8	1.8	114 (−88)	91 (−90)	623 (−92)	0.5 (−95)	+	1 (−96)	+++
D	II	ANME-1 (ANME-2)/DSS	0.6	4.8	103 (−92)	61 (−98)	395 (−100)	27 (−105)	+	6 (NA)	+++
E	II	NA	0.3	5.0	3 (−75)	1 (−76)	10 (−85)	tr (NA)	−	tr (−81)	+
F	II	ANME-1/DSS	0.2	17.3	214 (−78)	77 (−89)	226 (−91)	tr (−85)	−	18 (−90)	+++

Mat type I is black parts of the gas-filled globules at the top; mat type II is massive pink-orange mat. DSS, *Desulfusarcina/Desulfurococcus* group. Column 4 gives the ratios of hydroxyarchaeol to archaeol [(archaeol + *sn*-2-hydroxyarchaeol)/archaeol − 1]. Column 5 designates the ratios of phytane to the sum of biphytanes (C40:0 to C40:2) after the cleavage of ether bonds [(phytane + Σbiphytanes)/phytane − 1)]. Columns 6–12 give the concentrations, relative occurrences, and δ^{13}C values vs. VPDB, Vienna Pee Dee belemnite of selected archaeal lipids. arch, archaeol; OH-arch, *sn*-2-hydroxyarchaeol; Σbiph, sum of biphytanes; croc, crocetane; crocΔ, crocetenes, up to two double bonds; PMI, 2,6,10,15,19-pentamethylicosane; PMIΔ, unsaturated PMIs, up to five double bonds. The number of plus signs designates relative abundances. Detailed lipid compositions of the boldface samples are given in Figs. 2–4. tr, Traces; NA, not analyzed; ND, not detected.
*From FISH and TEM analyses.
†Sample described in ref. 8. Inconsistencies of the absolute concentrations of biphytanes and archaeol and the ratio given in column 5 are most likely a result of losses of absolute concentrations during the procedure of ether cleavage.

Results of other studies support the lipid-based distinction proposed here (8, 25–28). These studies mainly focused on the occurrence of certain strongly ^{13}C-depleted hydrocarbons (crocetane, PMI, and their unsaturated homologues) and isoprenoidal diethers (archaeol, *sn*-2- and *sn*-3-hydroxyarchaeol). High abundances of crocetane and *sn*-2-hydroxyarchaeol were observed in ANME-2-dominated samples [e.g., Hydrate Ridge, Oregon (9, 29), Guaymas basin core C (26); Table 2]. Moreover, the relative abundances of hydroxyarchaeol vs. archaeol at several ANME-2-dominated AOM sites show higher proportions of the hydroxylated dialkyl ether, which corroborates the results of this study (Table 2). So far, reports on intact tetraethers (GDGT) and/or ^{13}C-depleted biphytanes after cleavage of ether bonds exist only for ANME-1-dominated AOM sites (8, 27).

The observed distributions of lipids suggest different biosynthetic capabilities for ANME-1 and ANME-2 archaea. Specifically, the latter appear not to be capable of synthesizing internally cyclized GDGT. Support for this idea comes also from the absence of ^{13}C-depleted biphytanediols in a sediment core of the Guaymas basin (core C, mainly ANME-2 archaea) and the presence of these biomarkers in adjacent ANME-1-dominated cores (ref. 26 and Table 2).

The relatively high stability of archaeal lipids, especially crocetane, PMI, and biphytanes (except for hydroxyarchaeols), makes it possible to use lipid-biomarker criteria in studies of the fossil environment (32), to which molecular microbiological techniques cannot be applied. Depletions of ^{13}C in carbonate minerals and in distinctive microbial biomarkers have led to an association of several ancient sediments with AOM (33). For instance, a Jurassic seep carbonate from the French Beauvoisin Formation lacks crocetane but includes high concentrations of strongly ^{13}C-depleted biphytanes (33, 34). This pattern suggests that the main archaeal methanotrophs in the system were members of the ANME-1 cluster. In contrast, a tubeworm limestone from the Miocene Marmorito Formation contains high concentrations of crocetane and no biphytanes (33), which makes ANME-2 archaea the probable dominant methanotrophs in this paleoenvironment.

If the environmental parameters that favor growth of one consortium instead of the other can be identified, lipid-biomarker evidence will provide information about conditions in ancient environments.

Lipids and Phylogeny of ANME-1 and ANME-2. ANME-2 archaea are affiliated with the *Methanosarcinales* (28), a group of mainly methylotrophic methanogens belonging to the *Euryarchaeota*. In

Table 2. Relative proportions and occurrences of isoprenoidal dialkyl glycerol diethers, ether-bond biphytanes, and isoprenoidal hydrocarbons at recent AOM sites

Sample	Ref(s).	Major ANME cluster	(arch + OH-arch)/arch − 1	Biphytanes	Relative occurrence*			
					Crocetane	CrocetaneΔ	PMI	PMIΔ
Eel River PC 36 (4–7 cm)	28	ANME-2	2.08	NP	++	+	+++	++
Santa Barbara SB-pc24	28, 30	ANME-2	2.52	NP	+	NP	−	++
Guaymas core C	26	ANME-2	1.07	−†	NP	NP	NP	NP
Guaymas core T	26	ANME-2	0.78	−†	NP	NP	NP	NP
Hydrate Ridge	9, 29, 31	ANME-2	1.00	NP	+++	+	+++	++
Eel River ERB-Hpc4	25, 28, 30	ANME-1	0.25	NP	+	−	−	NP
Guaymas core A	26	ANME-1	0.05	++†	NP	NP	NP	NP
Napoli crust MN16BT2	27	ANME-1	0.20	+++	+	NP	+++	NP

Predominating AOM cluster, ratios of archaeol *vs.* *sn*-2-hydroxyarchaeol, and occurrences of archaeal lipids of selected AOM sites are tabulated. Note that the lipid data derive from free lipid extracts (not from hydrolysis). NP, not published.
*Relative occurrences of crocetane, unsaturated crocetenes (up to two double bonds), PMI, and unsaturated PMIs (up to five double bonds). Number of plus signs designates relative abundances. Minus sign denotes the absence of a compound.
†Internally cyclized biphytanediols.

contrast, ANME-1 form a separate cluster and are only distantly related to methanogens of the orders *Methanomicrobiales* and the *Methanosarcinales* (25). Unfortunately, no organism from either group has yet been isolated and grown in pure culture, so definite lipid inventories are not available. However, lipid compositions of various methanogenic archaea belonging to affiliated orders are well investigated. Strikingly, lipids of members of the order *Methanosarcinales* are mainly composed of isoprenoidal diethers such as archaeol and hydroxyarchaeol (*sn*-2 and *sn*-3), whereas members of the *Methanomicrobiales* lack hydroxyarchaeols but contain acyclic tetraether-bound biphytanes (35). Thus, our results support the hypothesis of a separation of the ANME-1 from the *Methanosarcinales* and may suggest a closer affinity to the *Methanomicrobiales*.

Ecological Implications from Lipids and Niches of AOM Communities. The lipid characteristics and habitats of ANME-1 and ANME-2 associations in the Black Sea bioherms may indicate their favored ecological conditions. Internally cyclized biphytanes are common within the phylum *Crenarchaeota*. Members of the *Crenarchaeota* were found in a microbial structure trawled from the anoxic bottom of the Black Sea (13). However, the application of a specific FISH probe showed only negligible contributions of *Crenarchaeota* to the microbial population of the mats investigated by us. Within the phylum *Euryarchaeota*, to which the ANME groups belong, internally cyclized biphytanes have been found only in hyperthermophilic members of the genera *Thermococcus* (36), *Thermoplasma* (37), and the methanogenic species *Methanopyrus kandlerii* (38). The presence of cyclopentyl units in tetraether-based lipids has been considered as important for an adaptation of these thermophilic microorganisms by increasing membrane stability in extreme environments (37). Indeed, archaeal methanotrophs capable of growing at temperatures higher than 90°C produce GDGTs (39). Therefore, the internally cyclized biphytanes in nonthermophilic members of the ANME-1 may be lipid-physiological relics from an ancestral thermophile. Moreover, *in vitro* experiments revealed that ANME-1 consortia are better adapted to elevated temperatures than ANME-2 (6). The occurrence and distribution of the different ANME groups in ancient oceans is still unclear, but the lipids produced by the ANME-1 group appear to qualify its members for growth over a wide range of temperatures.

Although associated SRB of both mats cluster in the *Desulfosarcina/Desulfococcus* group (Fig. 1 *E* and *F*), their lipid compositions differ remarkably (Fig. 4). The *ai*-C15:0 fatty acid is a prominent membrane constituent of *Desulfosarcina variabilis* and *Desulfococcus multivorans* (40). Affiliates of those organisms may therefore be present in the type II community (8). Fatty acids and acyl glycerides are, however, much more abundant in the type I mats. The C16:1ω5 and cycC17:0ω5,6 fatty acids found in this work are also abundant in a gas-hydrate-bearing sediment that apparently contains a type I community (9, 41). Remarkably high concentrations of bacterial DAGEs, observed here in the

type II community, have also been reported in a carbonate crust with abundant ANME-1 methanotrophs (20, 27). The temperatures in these environments are low, but the only cultivated organisms in which DAGEs have been found are thermophiles and deeply branching lineages such as *Thermodesulfobacterium commune* (42), *Thermodesulfobacterium hveragerdense* (43), *Aquifex pyrophilus* (44), and *Ammonifex degensii* (45). The presence of lipids otherwise found in thermophiles, a characteristic of the ANME-1 group, is, therefore, characteristic also of its syntrophic SRB partner in the type II community.

Support for a lesser degree of specialization of ANME-1 associations comes from microscopic analyses of AOM samples. The present observations, in accord with previous reports (5), show that ANME-2 archaea grow in close association with SRB, whereas ANME-1 archaea do not (Fig. 1 *E* and *F*). However, *in vitro* experiments indicate that both communities use methane and sulfate in a stoichiometry of about 1:1 (6). Thus, factors other than concentration of sulfate, such as partial pressures of methane, may induce preferential growth of ANME-1 or ANME-2. Notably, the present results show that ANME-2 are prevalent in parts of the Black Sea bioherms with presumably elevated methane partial pressure (mat type I).

In addition to the distributions and concentrations of archaeal biomarkers, Table 1 gives the $\delta^{13}C$ values of lipids found in the ANME-2- and ANME-1-dominated mats. Biomarkers from the methane-exposed type I mats are more strongly depleted in ^{13}C [compare archaeol in samples A and F, −99 and −78‰, respectively; $\delta^{13}C$ of methane −62.4 to −68.3‰ (8)]. A difference of ≈35‰ between the substrate methane and ANME-2 lipids and smaller depletions of ^{13}C in ANME-1 lipids have also been reported (5). However, it remains to be determined whether these differing values of $\delta^{13}C$ are due to different biosynthetic fractionations or to restrictions in the supply of methane to the secluded pink-orange mats. The comparatively high concentrations of prokaryotic biomarkers in the ANME-2-dominated parts of the Black Sea structures (Table 1) indicate considerably denser microbial populations in the methane-exposed compartments, possibly accompanied by high turnover rates.

Nevertheless, lipid differences between anaerobic methanotrophic communities allow for a distinction of ANME-1 and ANME-2 in recent and especially fossil sample sets, although mechanisms controlling the preferential growth need to be specified.

1. Barnes, R. O. & Goldberg, E. D. (1976) *Geology* **4,** 297–300.
2. Reeburgh, W. S. (1976) *Earth Planet. Sci. Lett.* **28,** 337–344.
3. Reeburgh, W. S., Whalen, S. C. & Alperin, M. J. (1993) in *Microbial Growth on C1 Compounds. Proceedings of the 7th International Symposium*, eds. Murrell, J. C. & Kelly, P. D. (Am. Soc. Microbiol., Washington, DC), pp. 1–14.
4. Valentine, D. L. (2002) *Antonie Leeuwenhoek* **81,** 271–282.
5. Orphan, V. J., House, C. H., Hinrichs, K.-U., McKeegan, K. D. & DeLong, E. F. (2002) *Proc. Natl. Acad. Sci. USA* **99,** 7663–7668.
6. Nauhaus, K., Treude, T., Boetius, A. & Krüger, M. (2004) *Environ. Microbiol.,* in press.
7. Nauhaus, K., Boetius, A., Krüger, M. & Widdel, F. (2002) *Environ. Microbiol.* **4,** 296–305.
8. Michaelis, W., Seifert, R., Nauhaus, K., Treude, T., Thiel, V., Blumenberg, M., Knittel, K., Gieseke, A., Peterknecht, K., Pape, T., *et al.* (2002) *Science* **297,** 1013–1015.

9. Boetius, A., Ravenschlag, K., Schubert, C. J., Rickert, D., Widdel, F., Gieseke, A., Amann, R., Jørgensen, B. B., Witte, U. & Pfannkuche, O. (2000) *Nature* **407,** 623–626.
10. Bohrmann, G., Ivanov, M., Foucher, J.-P., Spiess, V., Bialas, J., Greinert, J., Weinrebe, W., Abegg, F., Aloisi, G., Artemov, Y., *et al.* (2003) *Geo-Mar. Lett.* **23,** 239–249.
11. Wakeham, S. G., Lewis, C. M., Hopmans, E. C., Schouten, S. & Sinninghe Damsté, J. S. (2003) *Geochim. Cosmochim. Acta* **67,** 1359–1374.
12. Pimenov, N. V., Rusanov, I. I., Poglazova, M. N., Mityushina, L. L., Sorokin, D. Y., Khmelenina, V. N. & Trotsenko, Y. A. (1997) *Mikrobiologiya* **66,** 354–360.
13. Tourova, T. P., Kolganova, T. V., Kuznetsov, B. B. & Pimenov, N. V. (2002) *Mikrobiologiya* **71,** 230–236.
14. Kohnen, M. E. L., Schouten, S., Sinninghe Damsté, J. S., De Leeuw, J. W., Merritt, D. A. & Hayes, J. M. (1992) *Science* **256,** 358–362.

Blumenberg *et al.*

15. Elvert, M., Suess, E., Greinert, J. & Whiticar, M. J. (2000) *Org. Geochem.* **31,** 1175–1187.
16. Risatti, J. B., Rowland, S. J., Yon, D. A. & Maxwell, J. R. (1984) *Org. Geochem.* **6,** 93–104.
17. Schouten, S., van der Maarel, M. J. E. C., Huber, R. & Sinninghe Damsté, J. S. (1997) *Org. Geochem.* **26,** 409–414.
18. Teixidor, P. & Grimalt, J. O. (1992) *J. Chromatogr.* **607,** 253–259.
19. Hinrichs, K.-U., Pancost, R. D., Summons, R. E., Sprott, G. D., Sylva, S. P., Sinninghe Damsté, J. S. & Hayes, J. M. (2000) *Geochem. Geophys. Geosyst.* **1,** 10.1029/2000GC000042.
20. Pancost, R. D., Bouloubassi, I., Aloisi, G., Sinninghe Damsté, J. S. & the Medinaut Shipboard Party (2001) *Org. Geochem.* **32,** 695–707.
21. Manz, W., Arp, G., Schumann-Kindel, G., Szewzyk, U. & Reitner, J. (2000) *J. Microbiol. Methods* **40,** 125–134.
22. Manz, W., Eisenbrecher, M., Neu, T. R. & Szewzyk, U. (1998) *FEMS Microbiol. Ecol.* **25,** 43–61.
23. Burggraf, S., Mayer, T., Amann, R., Schadhauser, S., Woese, C. & Stetter, K. (1994) *Appl. Environ. Microbiol.* **60,** 3112–3119.
24. Sinninghe Damsté, J. S., Schouten, S., Hopmans, E. C., van Duin, A. C. T. & Geenevasen, J. A. J. (2002) *J. Lipid Res.* **43,** 1641–1654.
25. Hinrichs, K.-U., Hayes, J. M., Sylva, S. P., Brewer, P. G. & DeLong, E. F. (1999) *Nature* **398,** 802–805.
26. Teske, A., Hinrichs, K.-U., Edgcomb, V., de Vera Gomez, A., Kysela, D., Sylva, S. P., Sogin, M. L. & Jannasch, H. W. (2002) *Appl. Environ. Microbiol.* **68,** 1994–2007.
27. Aloisi, G., Bouloubassi, I., Heijs, S. K., Pancost, R. D., Pierre, C., Sinninghe Damsté, J. S., Gottschal, J. C., Forney, L. J. & Rouchy, J. M. (2002) *Earth Planet. Sci. Lett.* **203,** 195–203.
28. Orphan, V. J., Hinrichs, K.-U., Ussler, W., III, Paull, C. K., Taylor, L. T., Sylva, S. P., Hayes, J. M. & DeLong, E. F. (2001) *Appl. Environ. Microbiol.* **67,** 1922–1934.
29. Elvert, M., Suess, E. & Whiticar, M. J. (1999) *Naturwissenschaften* **86,** 295–300.
30. Hinrichs, K.-U., Summons, R. E., Orphan, V. J., Sylva, S. P. & Hayes, J. M. (2000) *Org. Geochem.* **31,** 1685–1701.
31. Elvert, M., Greinert, J., Suess, E. & Whiticar, M. J. (2001) in *Natural Gas Hydrates: Occurrences, Distribution, and Detection*, Geophysical Monograph Series, eds. Paull, C. K. & Dillon, W. P. (Am. Geophys. Union, Washington, DC), Vol. 124, pp. 115–129.
32. Thiel, V., Peckmann, J., Seifert, R., Wehrung, P., Reitner, J. & Michaelis, W. (1999) *Geochim. Cosmochim. Acta* **63,** 3959–3966.
33. Peckmann, J. & Thiel, V. (2004) *Chem. Geol.* **205,** 443–467.
34. Peckmann, J., Thiel, V., Michaelis, W., Clari, P., Gaillard, C., Martire, L. & Reitner, J. (1999) *Int. J. Earth Sci.* **88,** 60–75.
35. Koga, Y., Morii, H., Akagawa-Matsushita, M. & Ohga, M. (1998) *Biosci. Biotechnol. Biochem.* **62,** 230–236.
36. Lattuati, A., Guezennec, J., Metzger, P. & Largeau, C. (1998) *Lipids* **33,** 319–326.
37. Gambacorta, A., Trincone, A., Nicolaus, B., Lama, L. & De Rosa, M. (1994) *Syst. Appl. Microbiol.* **16,** 518–527.
38. Gattinger, A., Schloter, M. & Munch, J. C. (2002) *FEMS Microbiol. Lett.* **213,** 133–139.
39. Schouten, S., Wakeham, S. G., Hopmans, E. C. & Sinninghe Damsté, J. S. (2003) *Appl. Environ. Microbiol.* **69,** 1680–1686.
40. Kohring, L. L., Ringelberg, D. B., Devereux, R., Stahl, D. A., Mittelman, M. W. & White, D. C. (1994) *FEMS Microbiol. Lett.* **119,** 303–308.
41. Elvert, M., Boetius, A., Knittel, K. & Jørgensen, B. B. (2003) *Geomicrobiol. J.* **20,** 403–419.
42. Langworthy, T. A., Holzer, G., Zeikus, J. G. & Tornabene, T. G. (1983) *Syst. Appl. Microbiol.* **4,** 1–17.
43. Sturt, H. F., Summons, R. E., Smith, K., Elvert, M. & Hinrichs, K.-U. (2004) *Rapid Commun. Mass Spectrom.* **18,** 617–628.
44. Huber, R., Wilharm, T., Huber, D., Trincone, A., Burggraf, S., König, H., Rachel, R., Rockinger, I., Fricke, H. & Stetter, K. O. (1992) *Syst. Appl. Microbiol.* **15,** 340–351.
45. Huber, R., Rossnagel, P., Woese, C. R., Rachel, R., Langworthy, D. E. & Stetter, K. O. (1996) *Syst. Appl. Microbiol.* **19,** 40–49.

Blumenberg *et al.*